Optical anisotropies of asymmetric double GaAs (001) quantum wells

O. Ruiz-Cigarrillo [*], L. F. Lastras-Martínez,[†] E. A. Cerda-Méndez, G. Flores-Rangel,
C. A. Bravo-Velazquez, R. E. Balderas-Navarro, and A. Lastras-Martínez
Instituto de Investigación en Comunicación Óptica, Universidad Autónoma de San Luis Potosí
Alvaro Obregón 64, 78000 San Luis Potosí, S.L.P., México

N. A. Ulloa-Castillo
Tecnológico de Monterrey, School of Engineering and Science, Av. Eugenio Garza Sada Sur 2501, Monterrey, Nuevo León 64849, México

K. Biermann and P. V. Santos[‡]
Paul-Drude-Institut für Festkörperelektronik, Leibniz-Institut im Forschungsverbund Berlin e.V, Hausvogteiplatz 5-7, 10117, Germany

In the present work, we were able to identify and characterize a source of in-plane optical anisotropies (IOAs) occurring in asymmetric double quantum wells (DQWs), namely a reduction of the symmetry from D_{2d} to C_{2v} as imposed by asymmetry along the growth direction. We report on reflectance anisotropy spectroscopy (RAS) of double GaAs quantum well structures coupled by a thin (<2 nm) tunneling barrier. Two groups of DQW systems were studied: one where both QWs have the same thickness (symmetric DQW) and another where they have different thicknesses (asymmetric DQW). RAS measures the IOAs arising from the intermixing of the heavy and light holes in the valence band when the symmetry of the DQW system is lowered from D_{2d} to C_{2v}. If the DQW is symmetric, residual IOAs stem from the asymmetry of the QW interfaces, e.g., that associated with Ga segregation into the AlGaAs layer during the epitaxial growth process. In the case of an asymmetric DQW with QWs with different thicknesses, the AlGaAs layers (that are sources of anisotropies) are not distributed symmetrically at both sides of the tunneling barrier. Thus the system loses its inversion symmetry, yielding an increase in the RAS strength. The RAS line shapes were compared with reflectance spectra in order to assess the heavy- and light-hole mixing induced by the symmetry breakdown. The energies of the optical transitions were calculated by numerically solving the one-dimensional Schrödinger equation using a finite-difference method. Our results are useful for interpretation of the transitions occurring in both symmetric and asymmetric DQWs.

I. INTRODUCTION

Nanostructures based on double quantum wells (DQWs) constitute an excellent platform to study the interactions between confined energy levels, e.g., intra-QW transitions between electrons and holes belonging to the same QW (direct excitons and trions), and inter-QW transitions occurring for electrons and holes resident in different QWs (indirect excitons and indirect trions) [1]. The strength of the direct and indirect transitions can be modulated by the application of external perturbations, such as external electric fields. The electric field modifies the tunneling probability, leading to the appearance of spatially indirect inter-QW excitons [1–3] and intra-QW charged excitons (trions) [1]. Such complex band structures offer interesting optical phenomena that exhibit a polarization dependence. In-plane optical anisotropies (IOAs) of AlGaAs/GaAs-based heterostructure have been studied extensively in the past several years by means of reflectance anisotropy spectroscopy (RAS). In the case of single QWs, several sources of IOAs have been

investigated: (i) the absence of a fourfold rotational symmetry axis at the AlGaAs/GaAs interface [4,5], (ii) asymmetric quantum wells [6], (iii) nonuniform segregation of Ga atoms at AlGaAs/GaAs interfaces [5,7], (iv) application of an external stress [8,9], and (v) asymmetric barriers [10]. In general, the observed IOA strength depends on the QW thickness. For example, for strain-induced IOAs, the RAS response increases with the well thickness [8,9], whereas it decreases with the well thickness for the anisotropies induced exclusively by the interfaces [5,8,10].

In DQW-based systems, the relative thickness of the QWs plays an important role in the anisotropy strength; namely, if both QWs have the same thickness (symmetric DQW), the IOA arises from the contributions of the AlGaAs/GaAs(QW) and GaAs(QW)/AlGaAs interfaces, which, in general, are not equivalent. If the QW thicknesses are different (asymmetric DQW), the system loses its inversion symmetry as a whole along a plane perpendicular to the growth direction and passing through the center of the tunneling barrier; therefore, the interfaces of the DQW system are not distributed symmetrically at both sides of the tunneling barrier, leading to an increase of the IOA signal.

In this paper, we report on RAS experiments on DQWs coupled by a thin barrier (1.98 nm) and different relative thicknesses. We find that by increasing the thickness of one

[*]oscarruiz@cactus.iico.uaslp.mx
[†]lflm@cactus.iico.uaslp.mx
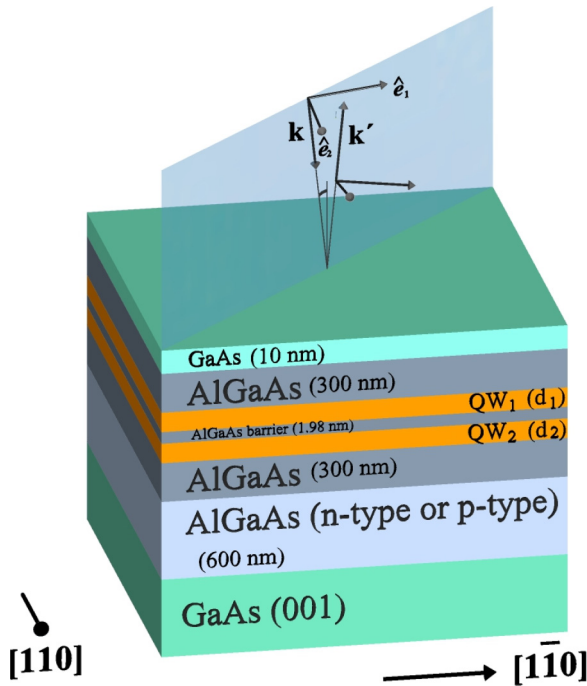[‡]santos@pdi-berlin.de

FIG. 1. Monochromatic light coming from a tungsten lamp is focused onto the (001) surface of the DQW structures. The angle of incidence is approximately $4°$. RAS spectra were obtained by taking the difference between the reflectance for $\hat{e}_1$ and $\hat{e}_2$ light polarizations. The experiments were performed at 30 K. Thicknesses d_1 and d_2 for the samples used in this work are listed in Table I.

of the QWs relative to the other, we induce a breakdown of inversion symmetry of the DQW structure, which increases the IOA.

The rest of the paper is organized as follows. In Sec. II, a description of samples and the experimental setup is given. In Sec. III, a description of the numerical model used to calculate the energy of the excitonic transitions of the DQWs and a detailed description of the model used to explain the RAS spectra are discussed. In Sec. IV, we describe the RAS and photoluminescence (PL) on symmetric and asymmetric DQWs as well as their interpretation on the basis of the breakdown of inversion symmetry. Finally, conclusions are given in Sec. V.

II. SAMPLES AND EXPERIMENTAL SETUP

The samples were grown by molecular beam epitaxy (MBE) on a GaAs (001) semi-insulating substrate covered with a 200-nm-thick smooth GaAs buffer layer (see Fig. 1 and Table I). On top of this layer, a 600-nm-thick, *n*-type

(samples S1, A1, and A2) or *p*-type (sample A3) $Al_{0.15}Ga_{0.85}As$ layer was grown. The DQW consists of two undoped GaAs QWs of thicknesses d_1 and d_2 separated by a 1.98-nm-thick $Al_{0.15}Ga_{0.85}As$ barrier. Sample S1 is a symmetric DQW (i.e., with $d_1 = d_2$) while samples A1, A2, and A3 are asymmetric ($d_1 \neq d_2$). The whole structure was covered with a 10-nm-thick GaAs capping layer.

RAS and reflectance (R) experiments were carried out using for excitation the monochromatic probe light obtained by filtering a 70 W tungsten lamp with a monochromator. The monochromatic beam then passes through a polarizer prism and a photoelastic modulator in tandem and is focused onto the sample with a spot size of 5.0 mm diameter. The sample is chilled at cryogenic temperatures (30 K) by means of a helium closed-cycle cryocooler. The light reflected by the sample is collected and detected by a multialkali photomultiplier tube. A detailed description of the RAS technique can be found elsewhere [11].

III. MODEL

A. Numerical calculations

The one-dimensional Schrödinger equation in the effective-mass approach was solved using the finite-difference method [12,13] to obtain both the transition energies and wave functions of the DQWs. We neglect spin-orbit interaction, which leads to a 4×4 Luttinger's Hamiltonian [14] with decoupled heavy- and light-hole states. Taking into account the band-edge variation $V(z)$ as well as the dependence of the effective mass $m(z)$ on the composition of the layers [13,15–17], our system can be described by

$$\left[-\frac{\hbar^2}{2m_{jz}} \frac{d^2}{dz^2} + V(z) \right] \psi_{nj}(z) = E_{nj}\psi_{nj}(z),$$
$$j = e, hh, lh. \quad (1)$$

The Varshni equation was employed for the determination of gap energies of $Al_xGa_{1-x}As$ alloys [18]. The conduction- and valence-band offsets were chosen as 65% and 35%, respectively. Both electron and hole effective masses for GaAs and AlAs can be found in Refs. [19–21], whereas for $Al_xGa_{1-x}As$ Vegard's law was used [22].

Figure 2 shows the energies and wave functions of the S1 [Fig. 2(a)] and A1 [Fig. 2(b)] samples calculated by the finite-difference model without band nonparabolicity. The transition energies were calculated by taking into consideration the exciton binding energy as a function of the well width [16,23]. We show that wave functions in an asymmetric DQW are asymmetrically distributed around the tunneling barrier for both electrons and holes. The barrier width plays an important role in tunneling. For a symmetric DQW, as noted above, the

TABLE I. Structure of samples used in this work.

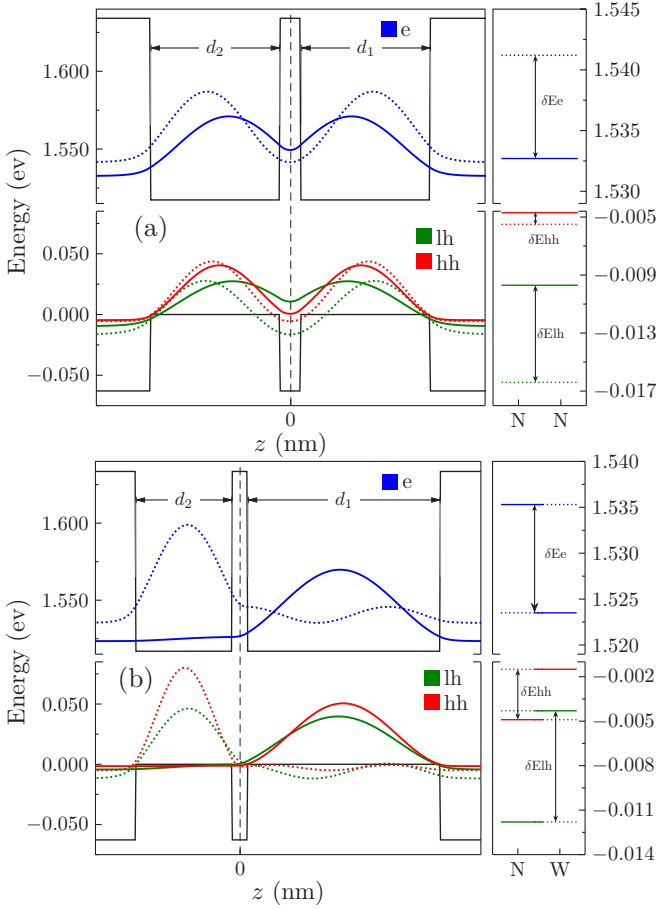| Sample number	Well width d_1 (nm)	Well width d_2 (nm)	$Al_{0.15}Ga_{0.85}As$
S1	11.87	11.87	Si doped, $n = 6 \times 10^{18}$ cm^{-3}
A1	13.85	11.87	Si doped, $n = 6 \times 10^{18}$ cm^{-3}
A2	23.74	11.87	Si doped, $n = 6 \times 10^{18}$ cm^{-3}
A3	23.74	11.87	Be doped, $p = 5 \times 10^{19}$ cm^{-3}

FIG. 2. Probability density functions (left panel) and confinement energies (right panel) for (a) sample S1 (symmetric DQW) and (b) sample A2 (asymmetric DQW).

electron and heavy- and light-hole states are quite similarly localized in the two wells and there is a splitting of the degenerate single states into doublets. For an asymmetric DQW the energies of doublets tend to the singlet state energy of a single QW [24].

B. Anisotropy model

GaAs is a cubic crystal of the symmetry group T_d. For a single QW grown on the (001) surface, the $z_\parallel(001)$ direction becomes inequivalent to both $x_\parallel(100)$ and $y_\parallel(010)$ directions, hence lowering symmetry from T_d to D_{2d}. This group comprises eight operations of symmetry, including four that change the direction of the z axis. In this symmetry group, the x and y axes remain equivalent and the optical properties are isotropic in the x-y plane. An IOA is expected when the $z_\parallel(001)$ axis loses its fourfold rotation symmetry, lowering the symmetry further from D_{2d} to C_{2v}. Different perturbations have been considered to increase the IOA; among them we can count on uniaxial external stress applied along the [110] direction, ultrathin layers inserted in one QW barrier, and external electric fields applied along the $z_\parallel(001)$ direction. Another mechanism that induces an IOA in a single QW is the nonequivalence of the AlGaAs/GaAs interfaces. As a matter of fact, in a single QW the anisotropies originated

at the AlGaAs/GaAs(QW) and at the GaAs(QW)/AlGaAs interfaces are reversed in sign, thus canceling the IOA (D_{2d} symmetry). However, it is well known that, experimentally, they are not exactly equivalent from a structural point of view [9], and a residual IOA is normally observed [4,5] (C_{2v} symmetry). RAS spectra of single QWs have been reported extensively in the literature [5,6,8–10].

The thickness of the QW plays a fundamental role in the amplitude of the RAS signal. For the anisotropies originating at the interfaces and the ones induced by the segregation of Ga or In (in the case of the inclusion of a thin InAs layer), the RAS amplitude decreases when the thickness of the QW increases [5]. Contrary to this behavior, for the IOA induced by strain, the RAS signal increases with the thickness of the QW [8]. In any case, the RAS signal is associated with the mixing between the heavy- and light-hole valence subbands of the QW [25]. In a perturbative approach, the IOA strength is proportional to

$$\frac{\langle\psi_{en}|\psi_{\text{hh}n}\rangle\langle\psi_{\text{hh}n}|\mathcal{H}|\psi_{\text{lh}n}\rangle\langle\psi_{\text{lh}n}|\psi_{en}\rangle}{\Delta E_n}, \qquad (2)$$

where $\langle\psi_{en}|\psi_{\text{hh}n}\rangle$ and $\langle\psi_{\text{lh}n}|\psi_{en}\rangle$ are the overlap integrals between the $|\psi_{en}\rangle$ electron state in the conduction band and the $|\psi_{\text{hh}n}\rangle$ and $|\psi_{\text{lh}n}\rangle$ hole states in the valence band, respectively. The mixing between heavy- and light-hole subbands is $\langle\psi_{\text{hh}n}|\mathcal{H}|\psi_{\text{lh}n}\rangle$, which is the perturbative Hamiltonian. The difference in energy between the hole states before their mixing is $\Delta E_n = E_{\text{hh}n} - E_{\text{lh}n}$.

As previously mentioned, $\mathcal{H}$ could account for a perturbation by applied uniaxial stresses, electric fields (built-in or external), and abrupt or smooth interfaces. In the case of a coupled DQW system, $\mathcal{H}$ is a measure of the asymmetry of the two QWs. In a DQW, if both QWs have the same thickness, the electron and hole energy levels are brought into resonance and their probability density is distributed symmetrically at both sides of the barrier that connects both QWs, as can be seen in Fig. 2(a). If the AlGaAs/GaAs interfaces of the DQW are equivalent, the symmetry of the DQW structure belongs to the D_{2d} crystallographic point group. However, as we mentioned, if the GaAs/AlGaAs interfaces (sources of anisotropies) are nonequivalent, a residual IOA is induced by the symmetry reduction from D_{2d} to C_{2v} of the whole DQW structure. In this case, the number of symmetry operations is reduced to four: the operations that invert the z-axis are excluded, thus leading to a mixing of heavy and light holes in the valence band, and hence an IOA.

When the thickness of one QW is larger than the other (asymmetric DQW), the energies of the electron and hole states of each QW become different and are no longer in resonance. In this case, the probability density is distributed asymmetrically, as can be seen in Fig. 2(b). In addition to the anisotropic source induced by the GaAs/AlGaAs interfaces as in the symmetric case, for the asymmetric DQW system another mechanism of IOA should be considered. Suppose that the AlGaAs/GaAs interfaces are equivalent. As we mentioned, in this case a symmetric DQW system belongs to the D_{2d} symmetry. If the thickness of one QW is modified, the system changes symmetry from D_{2d} to C_{2v}. As can be seen in Fig. 2(b), the symmetry operations that change the sign of the z-axis (i.e., a reflection on a plane perpendicular
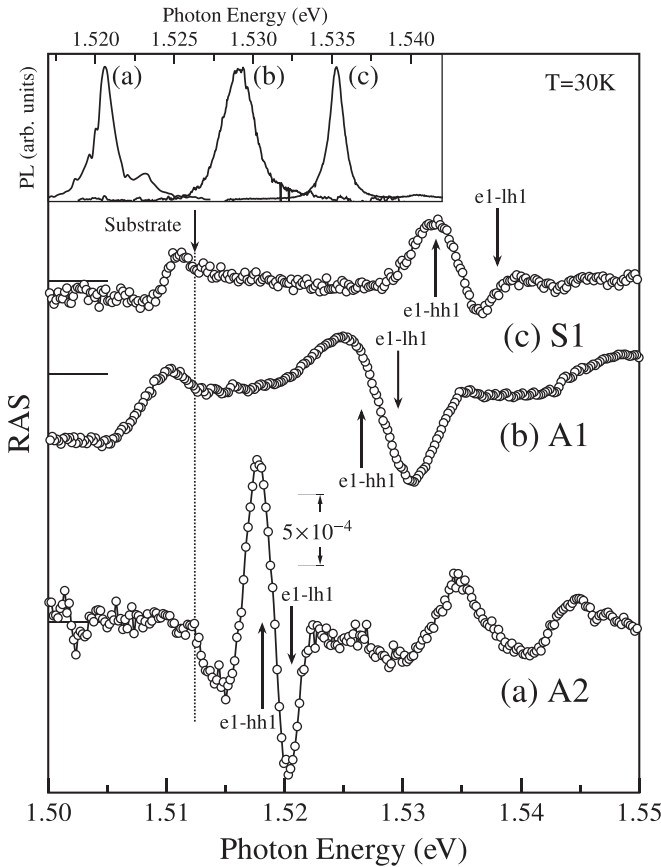
FIG. 3. RAS spectra for the (a),(b) asymmetric and (c) symmetric DQWs. The dashed vertical line indicates the expected energy of the excitonic transition of the GaAs substrate. Above this energy, the optical transitions come from the DQWs. The inset shows the PL spectra measured for each sample. Two peaks can be identified in each spectrum, a larger one associated with the transition $e1$-hh1 and a much smaller one associated with the $e1$-lh1 [for spectrum (b) this peak is observed as a shoulder]. The energies obtained from the PL spectra are indicated by the arrows in the RAS spectra. Note that the structures associated with $e1$-hh1 and $e1$-lh1 increase their strength when the DWQs become more asymmetric. The RAS spectra were measured at 30 K.

to z) are no longer possible because the AlGaAs/GaAs interfaces are located at different distances from the barrier. The number of symmetry operations of the asymmetric DQW structure is reduced to the four operations of the symmetry group C_{2v} [26,27]. In this case, the IOA strength can be modulated by changing the relative thicknesses of the QWs in the DQW system. This anisotropy is added to the residual IOA produced by the nonequivalence of the interfaces.

IV. EXPERIMENTAL RESULTS

Figure 3 shows the RAS spectra recorded at 30 K for samples S1, A1, and A2 (described in Table I). The inset show the corresponding PL spectra measured at 12 K, where the excitonic transitions can be identified by two peaks: the larger one associated with the $e1$-hh1 transition and a much smaller one associated with the $e1$-hh1 transition. In the case

of RAS, the peaks associated with these transitions are seen more clearly. The $e1$-hh1 and $e1$-lh1 transitions determined in the PL spectra are indicated by arrows. These values are in excellent agreement with those determined by the numerical calculations (see Table II). Note that the features associated with each transition have opposite concavities and redshift when one of the QWs of the system increases its thickness. The evolution of the optical structure is evident: if the DQW structure becomes asymmetric, the corresponding RAS spectra increase its strength.

Due to the fact that the wave-function probability density of sample S1 is distributed symmetrically along the QW structure, the IOA strength is expected to be similar to that obtained for a single QW. In fact, a RAS signal of the order of magnitude of 0.1×10^{-3} has been reported for an 8 nm single QW [5], which has the same order of magnitude as the spectra of Fig. 3(c). This IOA is attributed to the inequivalent AlGaAs/GaAs interfaces along the DQW structure.

As pointed out before, the strength of the IOA signal is produced by an intermixing of the heavy- and light-hole states in the valence band that is proportional to $\langle \psi_{\mathrm{hh}n} | \mathcal{H} | \psi_{\mathrm{lh}n} \rangle$ according to Eq. (2). For the lowest heavy- and light-hole levels ($n = 1$), there is an estimated separation in energy of around $\Delta E_1 = 2.0$, 4.1, and 4.4 meV for samples A2 (A3), A1, and S1, respectively. The mixing $\langle \psi_{\mathrm{hh}n} | \mathcal{H} | \psi_{\mathrm{lh}n} \rangle$ can be estimated by considering that the transitions are direct (n is the same for the valence and conduction band) and then the overlapping terms in Eq. (2) must be approximately the same for each sample. For transitions $n = 1$ it can be seen in Fig. 3 that the amplitude ratios of the spectra between A2 and A1 with respect to S1 are 1.5 and 3.7, respectively. Thus from Eq. (2) we estimate ratios of $\langle \psi_{\mathrm{hh}1} | \mathcal{H}_{\mathrm{A1}} | \psi_{\mathrm{lh}1} \rangle / \langle \psi_{\mathrm{hh}1} | \mathcal{H}_{\mathrm{S1}} | \psi_{\mathrm{lh}1} \rangle \sim 1.4$ for sample A1 and $\langle \psi_{\mathrm{hh}1} | \mathcal{H}_{\mathrm{A2}} | \psi_{\mathrm{lh}1} \rangle / \langle \psi_{\mathrm{hh}1} | \mathcal{H}_{\mathrm{S1}} | \psi_{\mathrm{lh}1} \rangle \sim 1.7$ for sample A2.

To elucidate the physical origin of the RAS in the asymmetric DQWs, we compare in Fig. 4 the RAS and the DR spectra of the asymmetric sample A2. DR spectra are obtained by numerical subtraction of the reflection (R) spectra recorded at 30 and 300 K followed by normalization to the 300 K spectrum. The subtraction highlights the excitonic features, which are very weak (and energy-shifted) at 300 K. The comparison between RAS and DR spectra allows us to contrast the contribution of the heavy- and light-hole transitions. Around 1.5175 eV, the DR spectrum shows two peaks corresponding to $e1$-hh1 and $e1$-lh1 transitions. Note that in the RAS spectrum, the structure associated with the $e1$-hh1 transition has the same concavity as the corresponding transition for the DR spectrum, while the $e1$-lh1 transition has the opposite concavity. This is an indication of the transfer of oscillator strength between the levels due to the intermixing of heavy and light holes, thus supporting our anisotropy model. The same behavior applies for the $e2$-hh2 and $e2$-lh2 transitions at around 1.5375 eV. Transition $e2$-hh3 is also indicated and it has the same concavity for RAS and DR spectra as in the case of the $e1$-hh1 and $e2$-hh2 transitions.

The arrows at the bottom of Fig. 4 indicate the energy of the states en-hh$n$ and en-lh$n$ (for $n = 1$ and 2) obtained from the maximum and minimum of the RAS spectrum. From the numerical calculation results summarized in Table II,

TABLE II. Comparative of experimental (E) and numerical (N) calculations of transition energies (in eV). δEe, δEhh, and δElh correspond to the difference between electron, heavy-, and light-hole states, respectively. ΔE_n is the numerical calculation of energy splitting for transitions 1 and 2 ($n = 1, 2$).

Sample	$e1$-hh1	$e1$-lh1	$e2$-hh2	$e2$-lh2	$e3$-hh3	δEe (meV)	δEhh (meV)	δElh (meV)	ΔE_n (meV)
S1	(E)1.5328 (N)1.5297	(E)1.5380 (N)1.5341	(N)1.5394	(N)1.5499	(N)1.5948	8.9	0.9	6.9	$\Delta E_1 = 4.4$ $\Delta E_2 = 10.5$
A1	(E)1.5265 (N)1.5273	(E)1.5296 (N)1.5314	(N)1.5368	(N)1.5460	(N)1.5837	8.4	1.3	6.4	$\Delta E_1 = 4.1$ $\Delta E_2 = 9.2$
A2	(E)1.5181 (N)1.5190	(E)1.5206 (N)1.5210	(N)1.5330	(N)1.5394	(N)1.5460	11.8	3.4	7.5	$\Delta E_1 = 2.0$ $\Delta E_2 = 6.4$

the energy splitting between transitions en-hh$n$ and en-lh$n$ is $\Delta E_1 = 2.0$ meV and $\Delta E_2 = 6.4$ meV, respectively. In accordance with Eq. (2), the IOA amplitude is proportional to $1/\Delta E_n$. Considering the same value for the overlapping and the mixing $\langle \psi_{\text{hh}n} | \mathcal{H} | \psi_{\text{lh}n} \rangle$, we estimate an amplitude ratio of
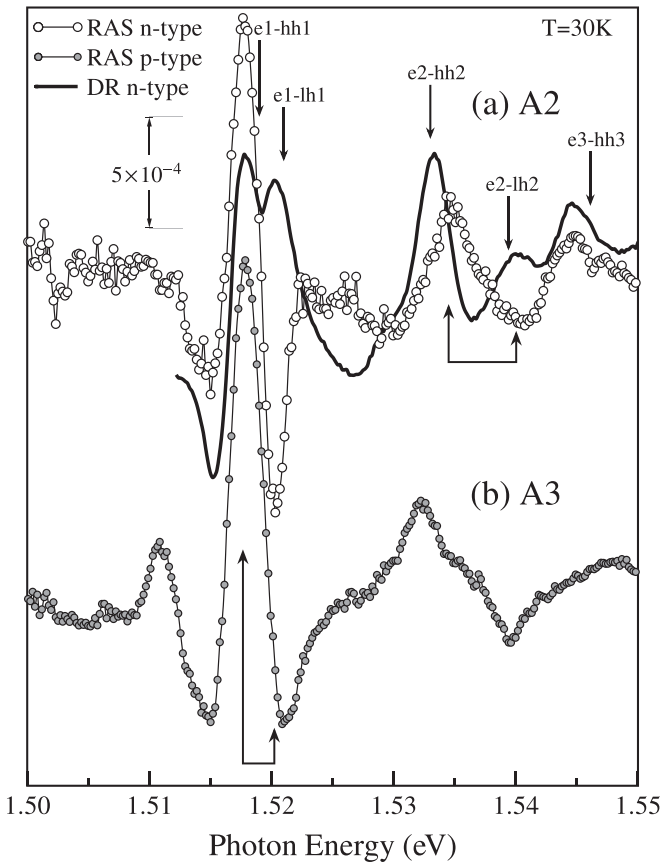

FIG. 4. Reflection anisotropy (RAS, open and closed circles) and differential reflection (DR, solid line) spectra for asymmetric DQWs A2 and A3, grown on an AlGaAs n-type and p-type layer, respectively. Note that while the heavy-hole transitions ($e1$-hh1 and $e2$-hh2) in the RAS and DR spectra have the same concavity, for the light-hole transitions ($e1$-lh1 and $e2$-lh2) the concavities are opposite, and DR spectra show the highest level transitions. The bottom arrows point to the experimental transitions for the two first levels, whereas the top arrows show the calculated energies to three energy levels. The RAS and DR spectra were measured at 30 K.

3.25 between these transitions. This value is close to the value of 3.9 obtained by the RAS spectrum of Fig. 4 supporting our interpretation.

Finally, we discuss the possible contribution to the RAS amplitude by a built-in electric field across the DQW. To study this contribution, we have compared the RAS spectra of asymmetric samples A2 and A3. The difference between them is the doping of the AlGaAs layer (see Fig. 1). While for A2 it is n-type, for A3 it is p-type. Assuming that the built-in electric field originates from charge transfer between surface states and the AlGaAs doped layer (n or p), this field is expected to have opposite signs for samples A2 and A3. Thus, the linear contribution of the electric field to the RAS should be reversed in sign for such samples. Figure 4 shows the comparison between the RAS spectra of samples A2 and A3 obtained from the difference in reflectivity between the [$1\bar{1}0$] and [110] crystallographic directions. As can be seen, RAS spectra are equivalent in shape and have the same sign, thus indicating that the contribution of the electric field to the RAS signal is very small. We thus conclude that the dominant contribution to RAS spectra is the asymmetry of the DQW system.

V. CONCLUSION

We presented in this work a detailed study of the evolution with QW thickness of the RAS spectra of a coupled DQW system. The RAS signal increases its strength with the degree of asymmetry of the QWs, which constitutes the DQW system. This behavior is attributed to the reduction of the symmetry of the electronic states in the DQWs with QWs of different thicknesses. The nature of the transitions was identified by using PL spectroscopy and numerical calculations. We believe that the results presented in this work are important and will be useful in understanding the evolution of the optical transition induced by the breakdown of translation symmetry in asymmetric DQWs.

[1] M. Yuan, A. Hernández-Mínguez, K. Biermann, and P. V. Santos, Tunneling blockade and single-photon emission in GaAs double quantum wells, Phys. Rev. B **98**, 155311 (2018).

[2] D. A. B. Miller, D. S. Chemla, T. C. Damen, A. C. Gossard, W. Wiegmann, T. H. Wood, and C. A. Burrus, Band-Edge Electroabsorption in Quantum Well Structures: The Quantum-Confined Stark Effect, Phys. Rev. Lett. **53**, 2173 (1984).

[3] Y. J. Chen, E. S. Koteles, B. S. Elman, and C. A. Armiento, Effect of electric fields on excitons in a coupled double-quantum-well structure, Phys. Rev. B **36**, 4562 (1987).

[4] O. Krebs and P. Voisin, Giant Optical Anisotropy of Semiconductor Heterostructures with no Common Atom and the Quantum-Confined Pockels Effect, Phys. Rev. Lett. **77**, 1829 (1996).

[5] Y. H. Chen, X. L. Ye, J. Z. Wang, Z. G. Wang, and Z. Yang, Interface-related in-plane optical anisotropy in GaAs/$Al_x$$Ga_{1-x}$As single-quantum-well structures studied by reflectance difference spectroscopy, Phys. Rev. B **66**, 195321 (2002).

[6] B. Koopmans, B. Koopmans, P. Santos, P. Santos, and M. Cardona, Microscopic reflection difference spectroscopy on semiconductor nanostructures, Phys. Status Solidi A **170**, 307 (1998).

[7] W. Braun, A. Trampert, L. Däweritz, and K. H. Ploog, Nonuniform segregation of Ga at AlAs/GaAs heterointerfaces, Phys. Rev. B **55**, 1689 (1997).

[8] C. G. Tang, Y. H. Chen, B. Xu, X. L. Ye, and Z. G. Wang, Well-width dependence of in-plane optical anisotropy in (001) GaAs/AlGaAs quantum wells induced by in-plane uniaxial strain and interface asymmetry, J. Appl. Phys. **105**, 103108 (2009).

[9] Y. Li, F. Liu, X. Ye, Y. Liu, J. Wang, and Y. Chen, Quantitative investigation of intrinsic shear strain and asymmetric interface conditions in semiconductor superlattices, J. Appl. Phys. **126**, 065704 (2019).

[10] J. L. Yu, S. Y. Cheng, Y. F. Lai, Q. Zheng, Y. H. Chen, and C. G. Tang, Tuning of in-plane optical anisotropy by inserting ultra-thin InAs layer at interfaces in (001)-grown GaAs/AlGaAs quantum wells, J. Appl. Phys. **117**, 015302 (2015).

[11] L. F. Lastras-Martínez, A. Lastras-Martínez, and R. E. Balderas-Navarro, A spectrometer for the measurement of reflectance-difference spectra, Rev. Sci. Instrum. **64**, 2147 (1993).

[12] Numerical solutions, *Quantum Wells, Wires and Dots* (Wiley, West Sussex, United Kingdom, 2016), Chap. 3, pp. 81–130.

[13] C. Hamaguchi, *Basic Semiconductor Physics* (Springer International, Cham, Switzerland, 2017).

[14] J. M. Luttinger, Quantum theory of cyclotron resonance in semiconductors: General theory, Phys. Rev. **102**, 1030 (1956).

[15] D. J. BenDaniel and C. B. Duke, Space-charge effects on electron tunneling, Phys. Rev. **152**, 683 (1966).

[16] Y. Takahashi, Y. Kato, S. S. Kano, S. Fukatsu, Y. Shiraki, and R. Ito, The effect of electric field on the excitonic states in coupled quantum well structures, J. Appl. Phys. **76**, 2299 (1994).

[17] L. C. Lew Yan Voon and M. Willatzen, Heterostructures: Basic formalism, in *The k p Method: Electronic Properties of Semiconductors* (Springer, Berlin, 2009), pp. 273–362.

[18] Y. P. Varshni, Temperature dependence of the energy gap in semiconductors, Physica **34**, 149 (1967).

[19] I. Vurgaftman, J. R. Meyer, and L. R. Ram-Mohan, Band parameters for iii-v compound semiconductors and their alloys, J. Appl. Phys. **89**, 5815 (2001).

[20] L. W. Molenkamp, R. Eppenga, G. W. 't Hooft, P. Dawson, C. T. Foxon, and K. J. Moore, Determination of valence-band effective-mass anisotropy in GaAs quantum wells by optical spectroscopy, Phys. Rev. B **38**, 4314 (1988).

[21] S. Adachi, *Properties of Semiconductor Alloys: Group-IV, III-V and II-VI Semiconductors* (Wiley, West Sussex, United Kingdom, 2009), Vol. 28.

[22] O. Donmez, F. Nutku, A. Erol, C. M. Arikan, and Y. Ergun, A study of photomodulated reflectance on staircase-like, n-doped GaAs/$Al_x$$Ga_{1-x}$As quantum well structures, Nanoscale Res. Lett. **7**, 622 (2012).

[23] R. L. Greene, K. K. Bajaj, and D. E. Phelps, Energy levels of Wannier excitons in GaAs $-$ $Ga_{1-x}$$Al_x$As quantum-well structures, Phys. Rev. B **29**, 1807 (1984).

[24] K. Sivalertporn, Effect of barrier width on the exciton states in coupled quantum wells in an applied electric field, Phys. Lett. A **380**, 1990 (2016).

[25] E. L. Ivchenko, A. Y. Kaminski, and U. Rössler, Heavy-light hole mixing at zinc-blende (001) interfaces under normal incidence, Phys. Rev. B **54**, 5852 (1996).

[26] E. L. Ivchenko and S. D. Ganichev, Spin-photogalvanics, in *Spin Physics in Semiconductors*, edited by M. I. Dyakonov (Springer, Berlin, 2008), pp. 245–277.

[27] M. Glazov, *Electron & Nuclear Spin Dynamics in Semiconductor Nanostructures*, Series on Semiconductor Science (Oxford University Press, Oxford, 2018).